

Gravitational Collapse of Thick Domain Walls

David Garfinkle

Dept. of Physics, Oakland University, Rochester, MI 48309, USA
and Michigan Center for Theoretical Physics, Randall Laboratory of Physics,
University of Michigan, Ann Arbor, MI 48109-1120, USA

E-mail: garfinkl@oakland.edu

Ryan Zbikowski

Dept. of Physics, Oakland University, Rochester, MI 48309, USA

E-mail: rmzbikow@oakland.edu

Abstract. Numerical simulations are performed of the gravitational collapse of a scalar field with a $\lambda\phi^4$ potential. Comparisons are made with the thin shell approximation.

1. Introduction

Domain walls in general relativity[1] are usually treated in the thin shell approximation.[2] However, there is also a description of a domain wall as a soliton of a field theory. In a certain limit one expects the field theory description to reduce to the thin shell description. Indeed, one can formally expand the Einstein-scalar equations in powers of the thickness and obtain the thin shell equations at lowest order in this expansion.[3, 4] Nonetheless, one cannot simply assume the validity of such an expansion. Instead in a field theory one gets to choose initial data and then the field equations give the results of the evolution of those data. Thus the thin shell approximation is a good approximation for a thick domain wall to the extent that the evolution of initial data that are well approximated by the thin shell treatment continue under evolution to be well approximated by this treatment. To test this approximation, we will choose initial data for a spherically symmetric thick domain wall, perform a numerical evolution, and compare to the corresponding thin shell approximation. Methods are described in section 2, results in section 3 and conclusions in section 4.

2. Methods

The Lagrangian for a thick wall takes the form

$$L = -\frac{1}{2}\nabla^a\phi\nabla_a\phi - V(\phi) \quad (1)$$

where $V(\phi)$ is a potential with two minima. The equation of motion associated with this Lagrangian is

$$\nabla^a\nabla_a\phi - \frac{dV}{d\phi} = 0 \quad (2)$$

The shell also satisfies the Einstein field equation

$$G_{ab} = \kappa T_{ab} \quad (3)$$

Here G_{ab} is the Einstein tensor, $\kappa = 8\pi G$ where G is Newton's gravitational constant, and the stress-energy of the scalar field is given by

$$T_{ab} = \nabla_a\phi\nabla_b\phi - \frac{1}{2}g_{ab}(\nabla^c\phi\nabla_c\phi + 2V) \quad (4)$$

Simulations of such thick walls in the case where their self-gravity can be neglected were done by[5] and [6]. We will use the standard $\lambda\phi^4$ potential

$$V = \lambda(\phi^2 - \eta^2)^2 \quad (5)$$

For simulations in spherical symmetry, one often takes the area radius as one of the spatial coordinates and chooses time to be orthogonal to this radial coordinate.[7] However, this coordinate system breaks down when a trapped surface forms and thus cannot follow the evolution after black hole formation. Instead we will use the method of [8] and use maximal slicing with radial length as the radial coordinate. Maximal slicing

allows us to simulate part of the region inside the black hole without encountering the singularity. The metric takes the form

$$ds^2 = -\alpha^2 dt^2 + (dr + \beta^r dt)^2 + R^2(d\theta^2 + \sin^2\theta d\varphi^2) \quad (6)$$

Note that the usual area radius R is not one of the coordinates and is instead a function of the coordinates t and r . Thus the spatial metric γ_{ab} has components

$$\begin{aligned} \gamma_{rr} &= 1 \\ \gamma_{\theta\theta} &= R^2 \\ \gamma_{\varphi\varphi} &= R^2 \sin^2\theta \end{aligned} \quad (7)$$

The extrinsic curvature, K_{ab} is defined by

$$K_{ab} = -\gamma_a^c \nabla_c n_b \quad (8)$$

where n^a is the unit normal to the surfaces of constant time t . However, due to spherical symmetry and maximal slicing, there is only one independent component of the extrinsic curvature. Specifically we have

$$K^\theta_\theta = K^\varphi_\varphi = -\frac{1}{2}K^r_r \quad (9)$$

Equation (8) is equivalent to

$$\partial_t \gamma_{ij} = -2\alpha K_{ij} + D_i \beta_j + D_j \beta_i \quad (10)$$

where D_i is the covariant derivative of the spatial metric γ_{ij} . The rr component of eqn (10) yields

$$\partial_r \beta^r = \alpha K^r_r \quad (11)$$

whose solution is

$$\beta^r = \int_0^r \alpha K^r_r dr \quad (12)$$

The $\theta\theta$ component of eqn (10) yields

$$\partial_t R = \beta^r \partial_r R + \frac{\alpha}{2} R K^r_r \quad (13)$$

We now use the momentum constraint of the Einstein field equation to determine the extrinsic curvature. For maximal slicing ($K = 0$) this constraint is

$$D_a K^{ab} = -\kappa \gamma^{bc} n^d T_{cd} \quad (14)$$

Define the quantities P and S by

$$P = n^a \nabla_a \phi, \quad S = \partial_r \phi \quad (15)$$

Then eqn (14) becomes

$$\partial_r K^r_r + 3R^{-1} K^r_r = -\kappa P S \quad (16)$$

Note that there is also a Hamiltonian constraint associated with the Einstein field equation. In the case of maximal slicing, this constraint is

$${}^{(3)}R - K_{ab} K^{ab} = 2\kappa T_{ab} n^a n^b \quad (17)$$

where ${}^{(3)}R$ is the spatial scalar curvature. This equation yields

$$\partial_r \partial_r R = \frac{1 - (\partial_r R)^2}{2R} - \frac{1}{4}R \left[\frac{3}{2}(K^r_r)^2 + \kappa(P^2 + S^2 + 2V) \right] \quad (18)$$

We now determine the lapse α . It follows from the maximal slicing condition that

$$D_a D^a \alpha = \alpha \left[K_{ab} K^{ab} + \frac{\kappa}{2} T_{ab} (n^a n^b + \gamma^{ab}) \right] \quad (19)$$

which yields

$$\partial_r \partial_r \alpha + \frac{2}{R} (\partial_r R) (\partial_r \alpha) = \alpha \left[\frac{3}{2} (K^r_r)^2 + \kappa (P^2 - V) \right] \quad (20)$$

We now consider the evolution of the scalar field. From the definitions of P and S it follows that

$$\partial_t \phi = \alpha P + \beta^r S \quad (21)$$

$$\partial_t S = \alpha (\partial_r P + K^r_r S) + P \partial_r \alpha + \beta^r \partial_r S \quad (22)$$

The equation of motion, eqn (2) becomes after some straightforward but tedious algebra

$$\partial_t P = \beta^r \partial_r P + S \partial_r \alpha + \alpha \left[R^{-2} \partial_r (R^2 S) - \frac{dV}{d\phi} \right] \quad (23)$$

The initial data are as follows: we choose a moment of time symmetry so that P and K_{ab} vanish. The scalar field ϕ is chosen to have a flat spacetime domain wall profile with the center of the wall at a radius r_0 . More precisely, define the quantities ϵ and σ by

$$\epsilon = \frac{1}{\eta \sqrt{2\lambda}} \quad (24)$$

$$\sigma = \frac{4}{3} \sqrt{2\lambda} \eta^3 \quad (25)$$

where η and λ are the parameters of the potential. Here σ is the energy per unit area of the wall and ϵ is an effective wall thickness. Formally the thin shell limit of the solution is the limit as $\epsilon \rightarrow 0$ at constant σ . Correspondingly, one can specify ϵ and σ ; then λ and η are determined by

$$\lambda = \frac{2}{3\sigma\epsilon^3} \quad (26)$$

$$\eta = \sqrt{\frac{3}{4}\sigma\epsilon} \quad (27)$$

In flat spacetime a static planar domain wall solution is given by

$$\phi = \eta \tanh(z/\epsilon) \quad (28)$$

We choose for initial data

$$\phi = \eta \tanh((r - r_0)/\epsilon) \quad (29)$$

where the constant r_0 can be chosen arbitrarily but should be chosen to be much larger than ϵ . The quantity S is set equal to $\partial_r \phi$. Eqn. (18) is integrated for R using the fact that at the origin $R = 0$ and $\partial_r R = 1$. Then at each time step, the evolution proceeds as follows: first eqns (16) and (18) are integrated to find K^r_r and R . And then eqn (20)

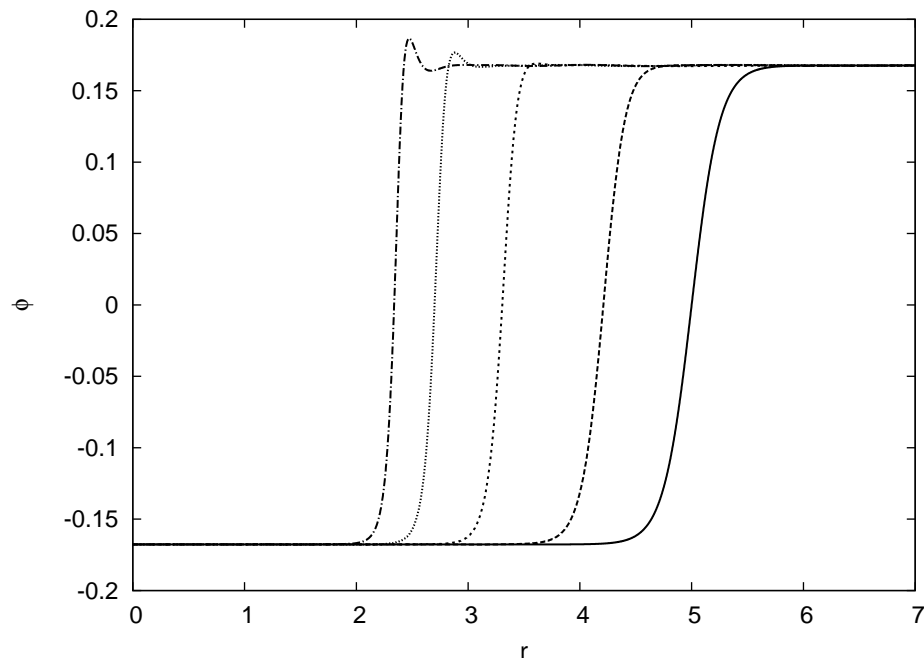


Figure 1. The scalar field ϕ at times 0, 2, 4, 6 and 8

is solved for the lapse α (using a tridiagonal method and the fact that $\partial_r \alpha = 0$ at the origin and $\alpha \rightarrow 1$ at infinity). Then eqn (12) is integrated to find the shift β^r . Finally, the quantities ϕ , S and P are evolved to the next time step using eqns (21), (22) and (23) respectively. The evolution is done using the iterated Crank-Nicholson method, and all spatial derivatives are found using standard centered differences. We use units where $\kappa = 1$.

As the evolution proceeds we can check for black hole formation by looking for the presence of a marginally outer trapped surface. In spherical symmetry, such a surface is given by the condition $\nabla^a R \nabla_a R = 0$ which in our coordinate system is equivalent to

$$\partial_r R + \frac{1}{2} R K^r_r = 0 \quad (30)$$

3. Results

The simulations are run with $n + 1$ points evenly spaced between $r = 0$ and a maximum value r_{\max} . We choose $r_{\max} = 20$. We would like to know how the initial scalar field profile changes under evolution. Fig 1 shows the result of a simulation with $r_0 = 5$, $\epsilon = 0.25$ and $\sigma = 0.15$. This simulation was run with $n = 9600$ and results are shown for the scalar field ϕ at times 0, 2, 4, 6, and 8. As the evolution proceeds, the scalar field profile moves inward. Furthermore, the profile becomes steeper, and departures from the simple tanh form become more pronounced. A marginally outer trapped surface forms at $t = 5.09$.

In order to be sure that these results are not numerical artifacts, we need to know that the code is convergent and that these results are within the convergent regime.

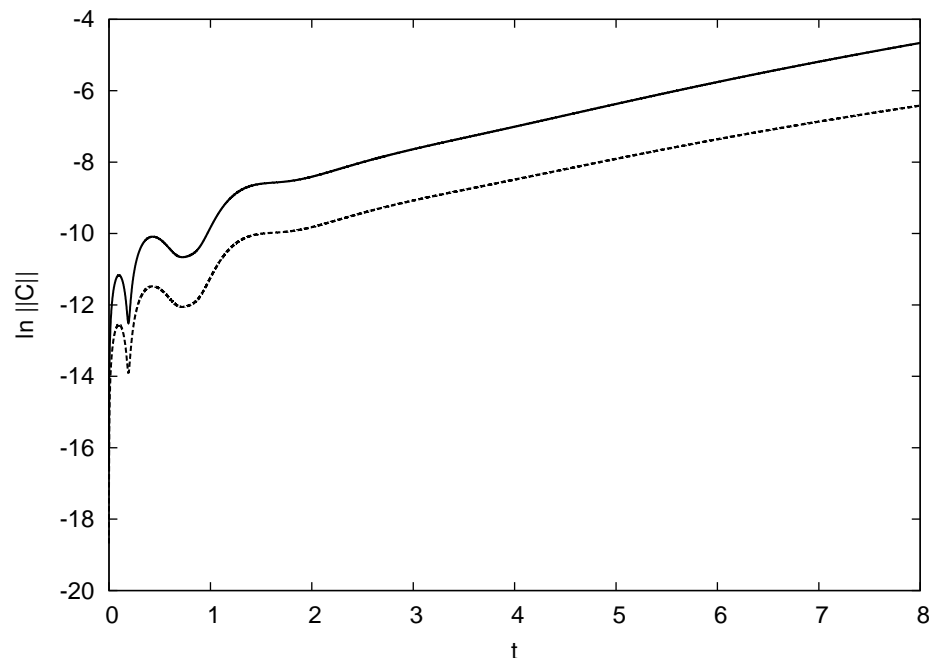


Figure 2. $\ln \|\mathcal{C}\|$ vs. t for $n = 9600$ (solid line) and $n = 19200$ (dashed line). The results demonstrate second order convergence.

Note that eqn. (13) is not used in the evolution, but should nonetheless be satisfied to within numerical error due to finite differencing. Thus this equation provides a check on the performance of the simulation. More precisely, define the constraint quantity \mathcal{C} by

$$\mathcal{C} = \frac{\alpha}{2} K^r_r + R^{-1}(\beta^r \partial_r R - \partial_t R) \quad (31)$$

and let $\|\mathcal{C}\|$ be the L_2 norm of \mathcal{C} . Then in an exact solution \mathcal{C} should vanish, while in a numerical treatment \mathcal{C} should converge to zero in the limit of zero step size. Fig 2 shows $\ln \|\mathcal{C}\|$ as a function of time. Here the parameters are as in the previous simulation, except that one simulation is run with $n = 9600$ and one with $n = 19200$. The results demonstrate second order convergence: that is, halving the step size reduces \mathcal{C} by a factor of 4.

In the thin shell formalism one is mostly concerned with the motion of the wall. The motion of a spherical wall is described by giving its area radius as a function of proper time. That is,

$$R = R_0(\tau) \quad (32)$$

Using the results of [1, 2] one can show that the equation of motion of the thin shell is

$$\ddot{R}_0 = \frac{3}{4} \kappa \sigma (1 + \dot{R}_0^2)^{1/2} - 2R_0^{-1} (1 + \dot{R}_0^2) \quad (33)$$

We would like to know how well the motion given by solving eqn. (33) models the behavior of the scalar field domain wall. Here we can do a direct comparison: at any given time, the position of the wall will be taken to be the place where $\phi = 0$ and the

proper time τ will be that of an observer who is always at the position of the wall. At each time step of the simulation, we can find the position of the wall, so it remains to evaluate τ . Let u^a be the four-velocity of the observer who remains at the position of the wall. Then it follows that u^a is a unit timelike vector for which $u^a \nabla_a \phi = 0$. It then follows using eqns (6) and (15) that

$$u^a = A^{-1} \left[n^a - \frac{P}{S} \left(\frac{\partial}{\partial r} \right)^a \right] \quad (34)$$

where the quantity A is defined by

$$A = \sqrt{1 - \frac{P^2}{S^2}} \quad (35)$$

evaluated at the position of the wall. The relation between the normal vector and the time coordinate is

$$n_a = -\alpha \nabla_a t \quad (36)$$

so using eqn. (34) we have

$$\frac{dt}{d\tau} = u^a \nabla_a t = -\alpha^{-1} u^a n_a = \alpha^{-1} A^{-1} \quad (37)$$

and therefore we find

$$d\tau = \alpha A dt \quad (38)$$

Choosing $\tau = 0$ at the beginning of the simulation, we then integrate eqn. (38) to find τ at all times of the simulation. Since we also have R_0 at all points of the simulation, we can produce the thick wall $R_0(\tau)$ for comparison with the $R_0(\tau)$ of the thin wall. Fig. (3) shows such a comparison. Here the parameters of the wall are the same as in the previous simulations, with the solid line being that of the simulation and the dashed line the solution of eqn. (33).

We now consider a comparison of the stress-energy of the simulation to that of the thin shell approximation. From eqns (4) and (15) it follows that the trace of the stress-energy tensor is

$$T = P^2 - S^2 - 4V \quad (39)$$

However, in the treatment of [3] to lowest order in thickness of the wall we have

$$T = \frac{-9\sigma}{4\epsilon \cosh^4(z/\epsilon)} \quad (40)$$

where z is geodesic distance from the center of the wall. Calculating geodesic distance from a simulation can be complicated; but luckily because the expression for T in eqn. (40) falls off so rapidly, we only need z in the vicinity of the wall's center and thus can approximate z using a Taylor series. In particular, note that at the center of the wall $\nabla_a z$ must be a unit vector orthogonal to u^a . It then follows that

$$\nabla^a z = A^{-1} \left[\left(\frac{\partial}{\partial r} \right)^a - \frac{P}{S} n^a \right] \quad (41)$$

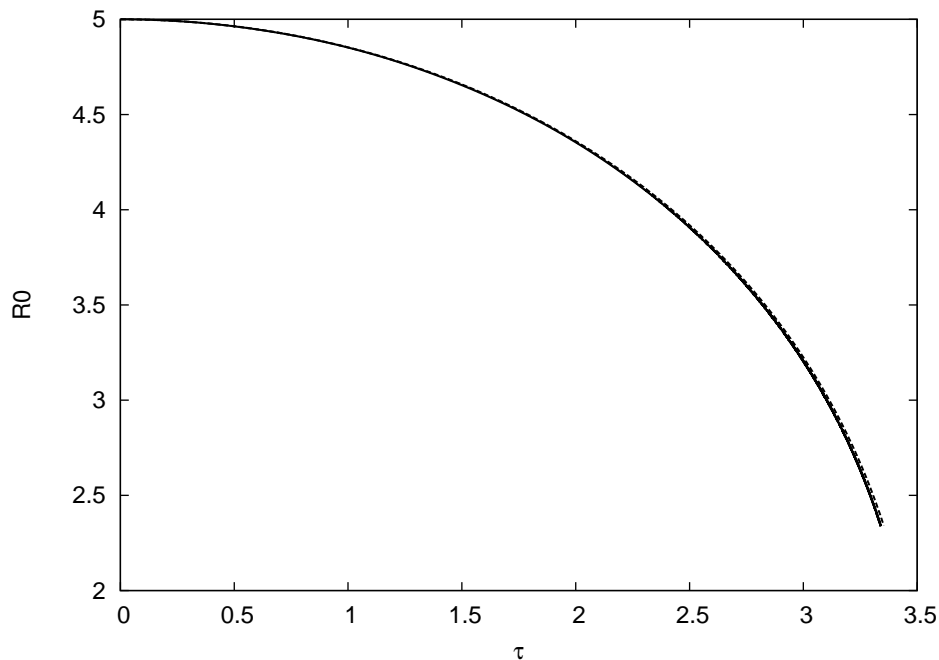


Figure 3. R_0 vs. τ for the simulation (solid line) and the thin wall equations of motion (dashed line).

Taking the inner product of eqn. (41) with $(\partial/\partial r)^a$ we find that at the center of the wall

$$\frac{\partial z}{\partial r} = A^{-1} \quad (42)$$

and we therefore find that near the wall z is well approximated by

$$z = (r - R_0)/A \quad (43)$$

Thus the thin wall expression for T is given by eqn. (40) with z given by eqn. (43).

Such a comparison is given in Fig (4) for $t = 2$ and in Fig (5) for $t = 6$. The parameters of the wall are the same as in the previous simulations. Here the trace of the stress-energy T is plotted for the simulation (solid line representing the expression of eqn. (39)) and for the thin shell approximation (dashed line representing the expression of eqn. (40)). Note that the simulation results are well approximated by the thin shell expression, though the approximation becomes less good as the evolution proceeds.

4. Conclusions

Our simulations indicate that the thin wall approximation is an excellent approximation for thick wall gravitational collapse. Perhaps more importantly, we have developed a robust numerical method for thick wall collapse that could be used on other projects. In particular, we plan to simulate the collapse of a charged thick domain wall. Thin charged walls collapse to charged black holes and can even be used to form an extreme (charge equals mass) black hole.[9] In contrast, simulations of the collapse of a free

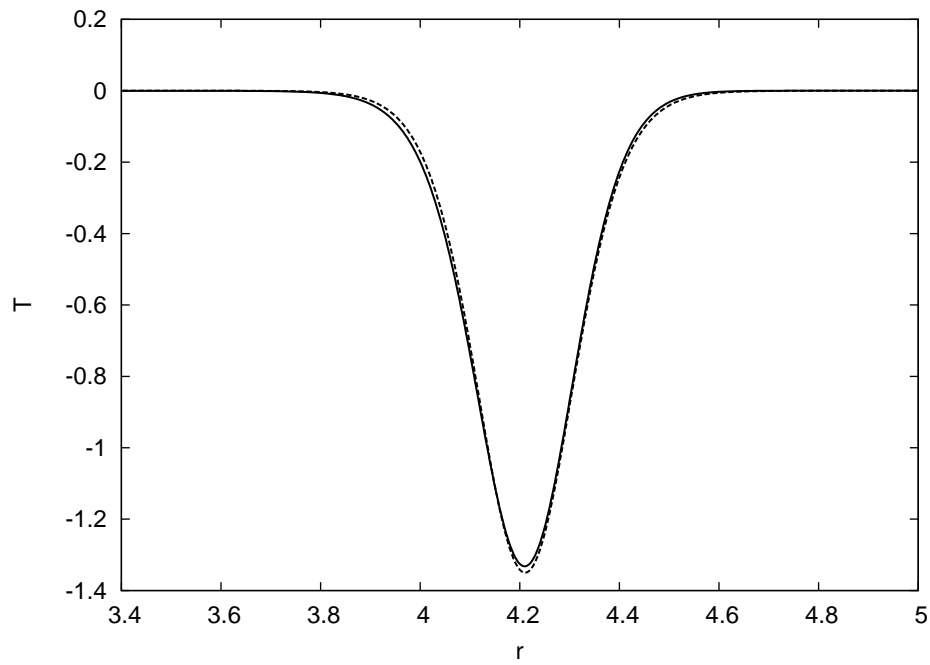


Figure 4. T vs. r at $t = 2$ for the simulation (solid line) and the thin wall approximation (dashed line).

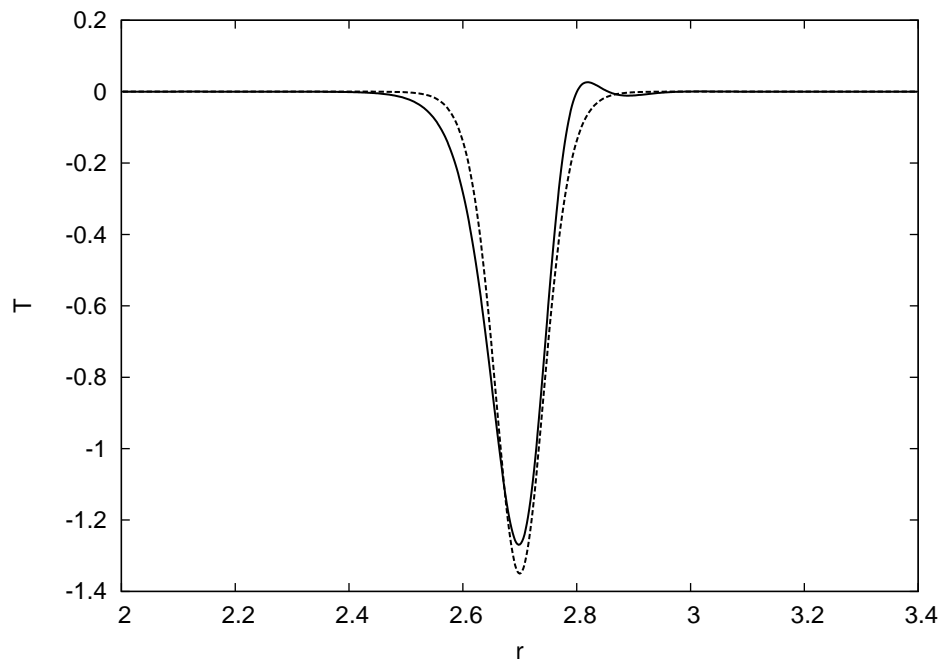


Figure 5. T vs. r at $t = 6$ for the simulation (solid line) and the thin wall approximation (dashed line).

charged scalar field yield black holes that are always far from extreme.[10] It will be interesting to see whether an extreme black hole can be formed by the collapse of a charged thick domain wall.

Acknowledgments

This work was supported by NSF grant PHY-0855532 to Oakland University.

References

- [1] Ipser J and Sikivie P 1984 *Phys. Rev.* **D30** 712
- [2] Israel W 1966 *Nuovo Cimento* **44B** 1
- [3] Garfinke D and Gregory R 1990 *Phys. Rev.* **D41** 1889
- [4] Gregory R, Haws D, and Garfinkle D 1990 *Phys. Rev.* **D42** 343
- [5] Widrow L 1989 *Phys. Rev.* **D40** 1002
- [6] Press W, Ryden B, and Spergel D 1989 *Astrophys. J.* **347** 590
- [7] Choptuik M, *Phys. Rev. Lett.* 1993 **70** 9
- [8] Akhoury R, Garfinkle D, and Saotome R 2011 *JHEP* **1104** 096
- [9] de la Cruz V and Israel W 1967 *Il Nuovo Cimento* **51** 744
- [10] Hod S and Piran T 1997 *Phys. Rev. D* **55** 3485